Science Immunology
AAAS

Supplementary Materials for

Long 3′UTRs predispose neurons to inflammation by promoting immunostimulatory double-stranded RNA formation

Tyler J. Dorrity *et al.*

Corresponding author: Hachung Chung, hc3070@cumc.columbia.edu

Sci. Immunol. **8**, eadg2979 (2023)
DOI: 10.1126/sciimmunol.adg2979

The PDF file includes:

Other Supplementary Material for this manuscript includes the following:

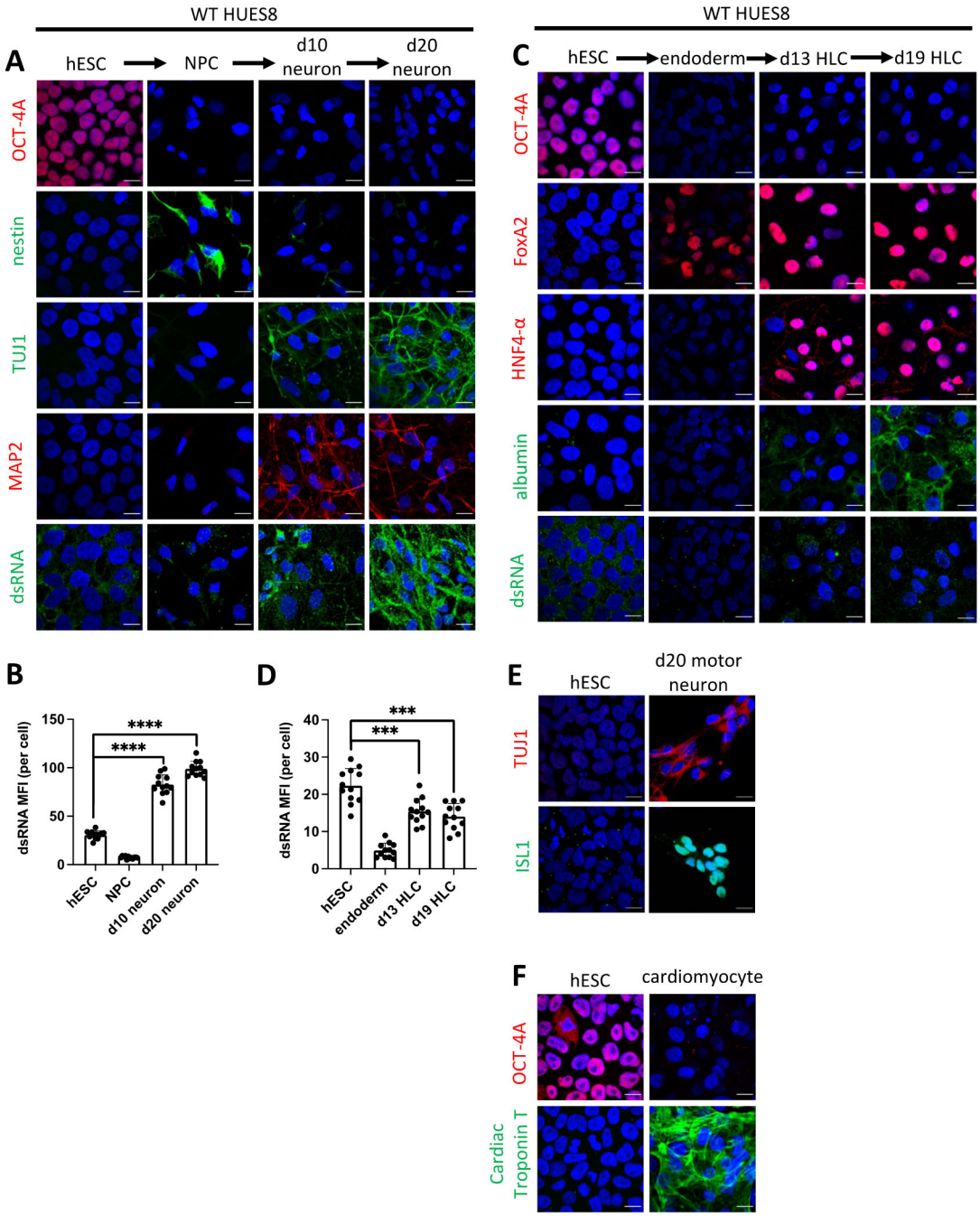

Fig. S1. Generation of diverse human cell types from HUES8 hESCs. (**A-B**) Immunofluorescence assay showing neuronal differentiation of WT hESCs (human embryonic stem cell) and dsRNA levels. hESC line, HUES8. Cells stained for a hESC marker (OCT-4A), a neural progenitor cell (NPC) marker (nestin), neuron markers (TUJ1 and MAP2), and dsRNA (J2 antibody) (A). Bar graph quantifying dsRNA signal from individual cells across multiple images (B). (**C-D**) Immunofluorescence assay of showing differentiation of HUES8 hESCs into hepatocyte-like cells (HLC) and dsRNA levels. Cells stained for a hESC marker (OCT-4A), a endoderm-lineage marker (FoxA2), a hepatocyte-lineage marker (HNF4-α), a marker of mature

hepatocytes (albumin), and dsRNA (J2 antibody) (C). Bar graph quantifying dsRNA signal from individual cells across multiple images (D). (**E**) Immunofluorescence assay showing hESC (HUES8) differentiation to day 20 (d20) motor neurons. Cells stained for a general neuron marker (TUJ1) and a motor neuron specific marker (ISL1). (**F**) Immunofluorescence assay showing hESC (HUES8) differentiation to cardiomyocytes. hESC and cardiomyocytes stained for a hESC marker (OCT-4A) and a cardiomyocyte marker (Cardiac Troponin T). All quantified data shown are mean ± S.D (n=12). (B,D) One-way ANOVA with Tukey corrected multiple comparisons, *$p < 0.05$, **$p < 0.01$, ***$p < 0.001$, ****$p < 0.0001$. Scale bars represent 10μm.

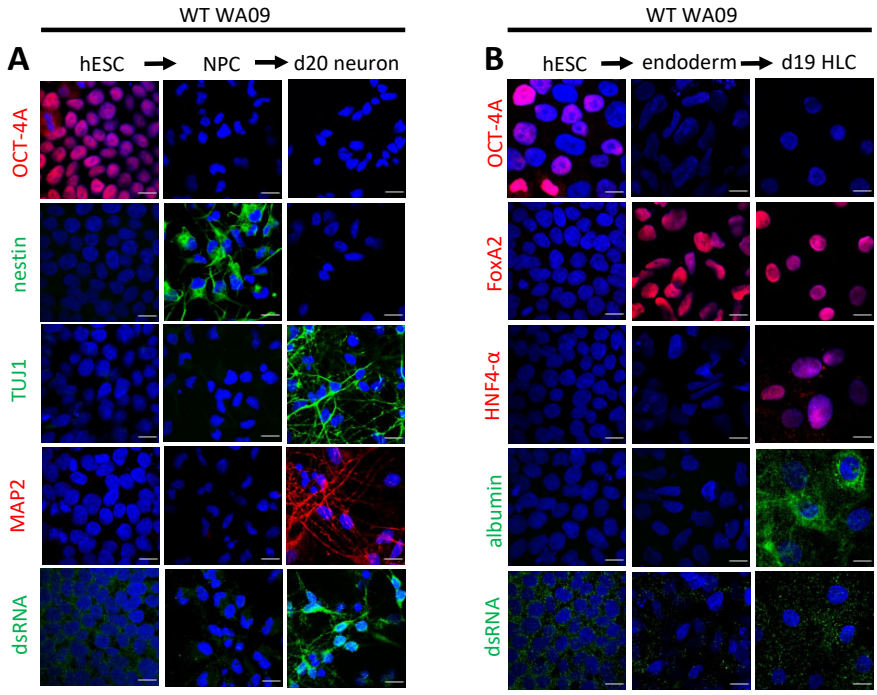

Fig. S2. Comparison of dsRNA levels between neurons and HLCs derived from WA09 hESCs. (**A-B**) WA09 hESCs differentiated to day 20 (d20) neurons (A) or day 19 (d19) hepatocyte-like cells (HLCs) (B). Immunofluorescence staining demonstrating neuronal differentiation (A). hESC marker, OCT-4A; neural progenitor cell (NPC) marker, nestin; neuron markers, TUJ1 and MAP2; dsRNA stained with the J2 antibody (A). Immunofluorescence staining demonstrating HLC differentiation (B). hESC marker, OCT-4A; endoderm-lineage marker, FoxA2; hepatocyte-lineage marker, HNF4-α; mature hepatocyte marker, albumin; dsRNA stained with the J2 antibody (B). Scale bars represent 10μm.

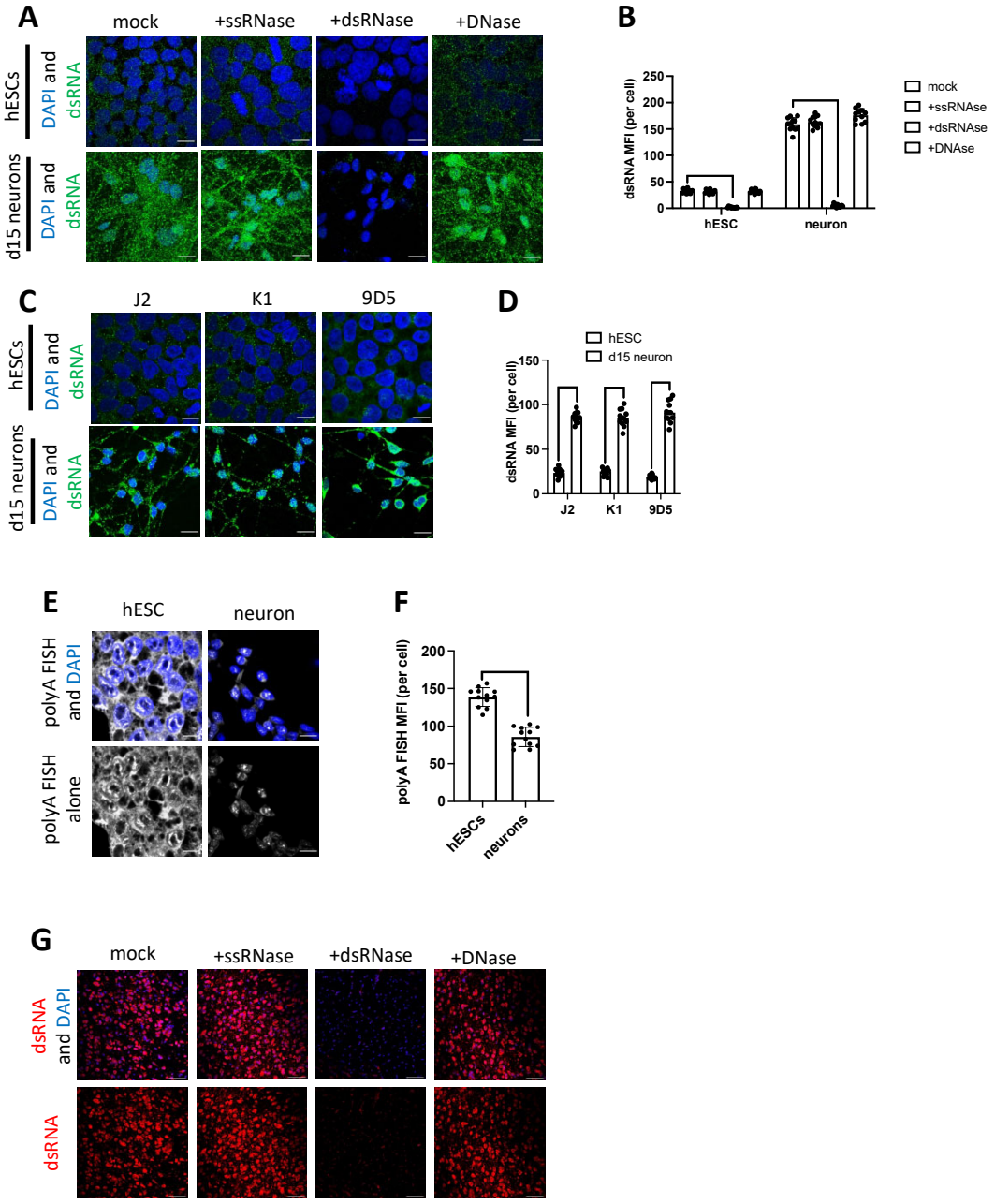

Fig. S3. Series of experiments to validate dsRNA enrichment in neurons. (**A-B**) Immunofluorescence images of hESCs (HUES8) and day 15 (d15) neurons treated with RNase T1 (ssRNase, 100U/mL), RNase III (dsRNase, 40U/L), or DNase (DNase, 40U/L) for 30 minutes and stained for dsRNA (J2 antibody, green) and nuclei (DAPI, blue) (A). dsRNA MFI plotted in bar graphs demonstrate that the J2 signal is specifically diminished upon dsRNase treatment (B). (**C-D**) Immunofluorescence images of hESCs (HUES8) and d15 (day 15) neurons stained for dsRNA with various anti-dsRNA antibodies: J2, K1, or 9D5 (C). For all antibodies, dsRNA MFI plotted in bar graphs show that neurons have more dsRNA than hESCs (D). (**E-F**) mRNA levels between hESC and day 15 neurons assessed by conducting FISH (Fluorescence In Situ Hybridization) for

polyA RNAs. Images of DAPI (blue) and polyA FISH (mRNA, white) staining (E). Quantification of polyA FISH signal (F). (**G**) Mouse cerebral cortex treated with indicated nucleases and stained with the 9D5 antibody (dsRNA, red). All bar graphs are mean ± S.D (n=12). (B) One-way ANOVA with Tukey corrected multiple comparisons, (D, F) Student's T-test, *p < 0.05, **p < 0.01, ***p < 0.001, ****p < 0.0001. All scale bars represent 10μm except for (G), which is 50μm.

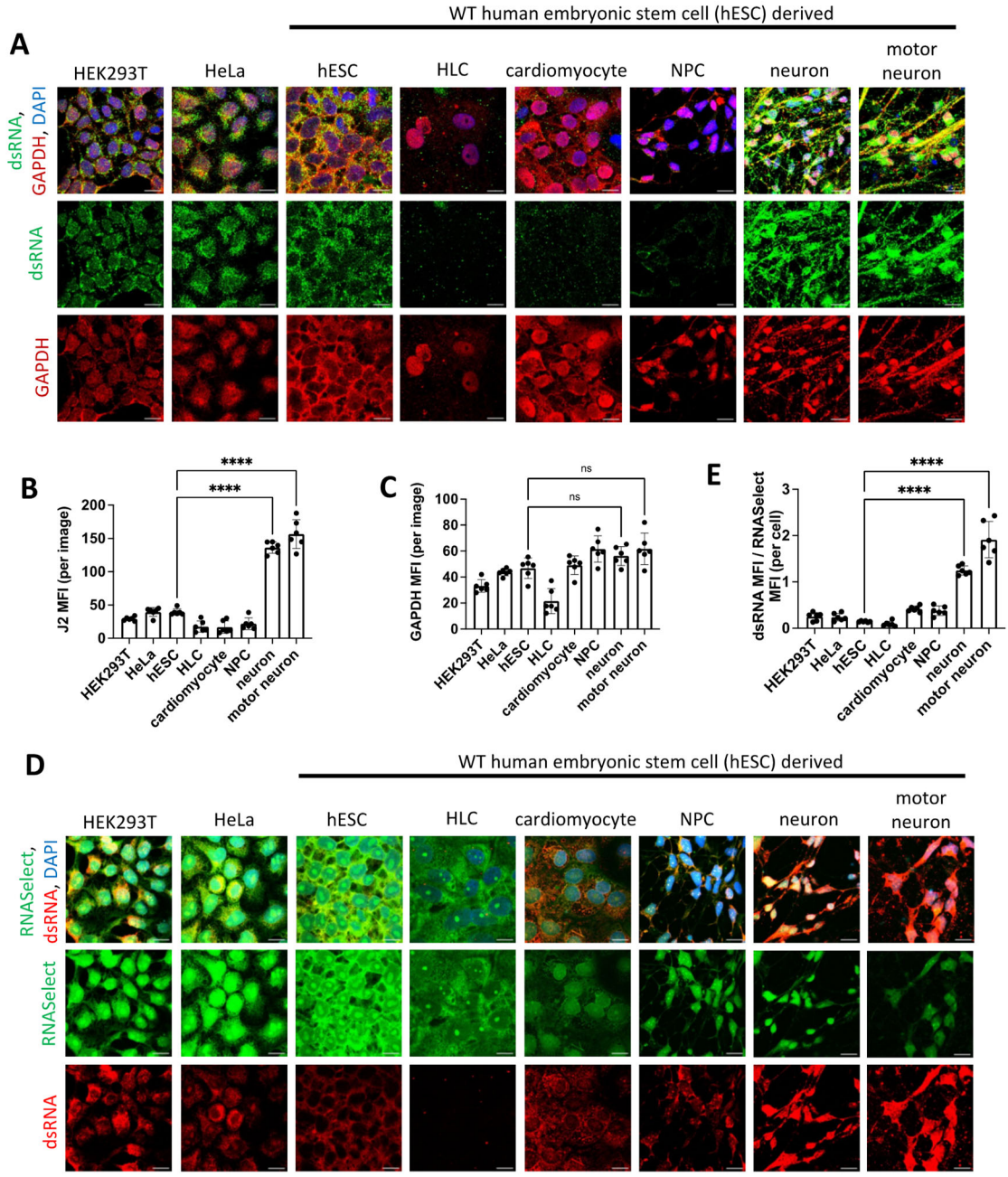

Fig. S4. Staining for dsRNA, GAPDH, and total RNA across multiple cell types. (**A-C**) Comparison of dsRNA and GAPDH levels across multiple human cell types. Cells stained with DAPI (blue), J2 immunostaining (dsRNA, green), and GAPDH (red). (B) MFI quantification of dsRNA in (A). (C) MFI quantification of GAPDH in (A). (**D-E**) Comparison of dsRNA and total RNA levels across multiple human cell types. Cells stained with DAPI (blue), 9D5 immunostaining (dsRNA, red), and RNASelect (green). (E) Quantification of dsRNA signal normalized to total RNA signal in (D). All bar graphs are mean ± S.D (n=6). One-way ANOVA with Tukey corrected multiple comparisons. *$p < 0.05$, **$p < 0.01$, ***$p < 0.001$, ****$p < 0.0001$. All scale bars represent 10µm.

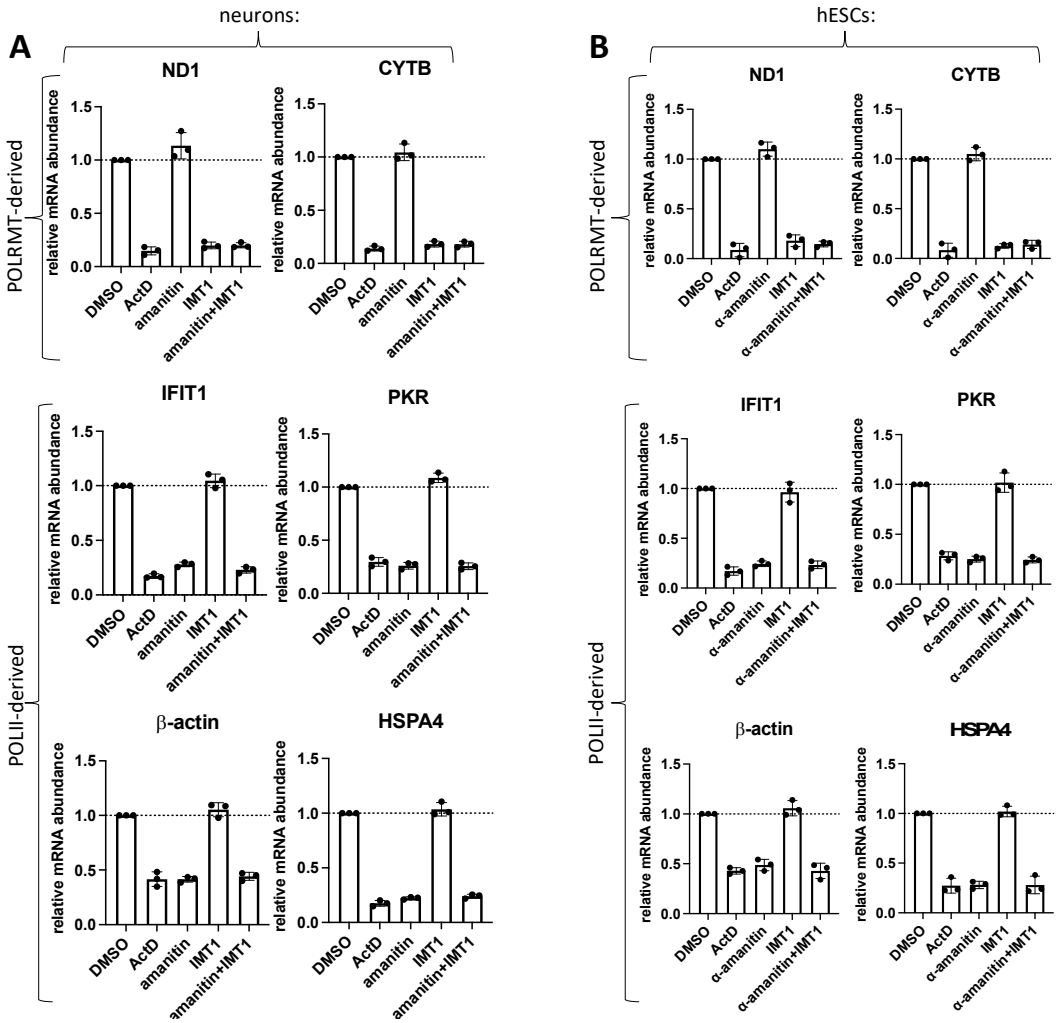

Fig. S5. Validating the specificity of RNA polymerase inhibitors. (**A-B**) Neurons or hESCs (HUES8) treated for 12 hours with the various RNA polymerase inhibitors or DMSO control. Actinomycin-D (ActD, 10 μg/mL) inhibits both RNA polymerase II (POLII) and mitochondrial transcription; α-amanitin (25 μg/mL) is a POLII inhibitor; IMT1 (1 μM) is a mitochondrial RNA polymerase (POLRMT) specific inhibitor. qPCR was conducted to confirm specificity of each inhibitor. Levels of POLII-derived transcripts (*IFIT1*, *PKR*, *β-actin*, *HSPA4*) and POLRMT-derived transcripts (*ND1*, *CYTB*) normalized to *RPS11* transcript in neurons (A) and hESCs (B). Data are shown as mean ± S.D (n=3).

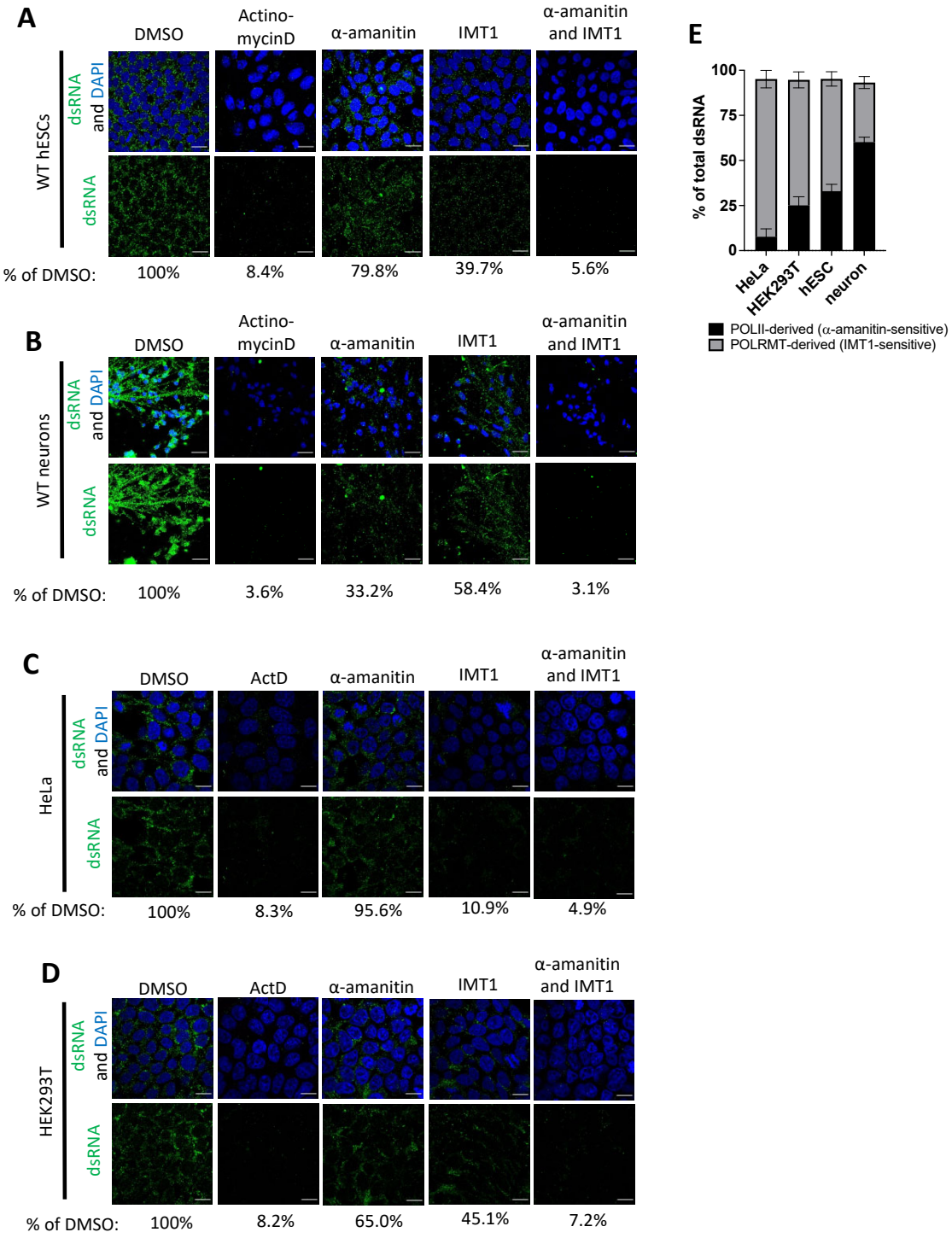

Fig. S6. Defining the origin of dsRNAs in diverse cell types. (**A-D**) hESCs, neurons, HeLa, and HEK-293T cells were treated with various RNA polymerase inhibitors or DMSO for 12 hours, and then underwent immunofluorescent imaging. Actinomycin-D (ActD, 10 μg/mL) inhibits both RNA polymerase II (POLII) and mitochondrial transcription; α-amanitin (25 μg/mL) is a POLII inhibitor; IMT1 (1 μM) is a mitochondrial RNA polymerase (POLRMT) specific inhibitor. J2 antibody (dsRNA, green) and DAPI (blue). Percentages indicate the

percentage of dsRNA MFI of each image compared to the dsRNA MFI in DMSO-treated sample. (**E**) HeLa, HEK-293T, hESCs, and neurons were treated with either α-amanitin or IMT1 and had dsRNA levels determined by J2 immunofluorescence as shown in A-D. Proportion of POLII-derived or POLRMT-derived transcripts calculated by determining the loss in dsRNA signal upon treatment with α-amanitin or IMT1, respectively. Data are shown as mean (n=3). Scale bars represent 10μm.

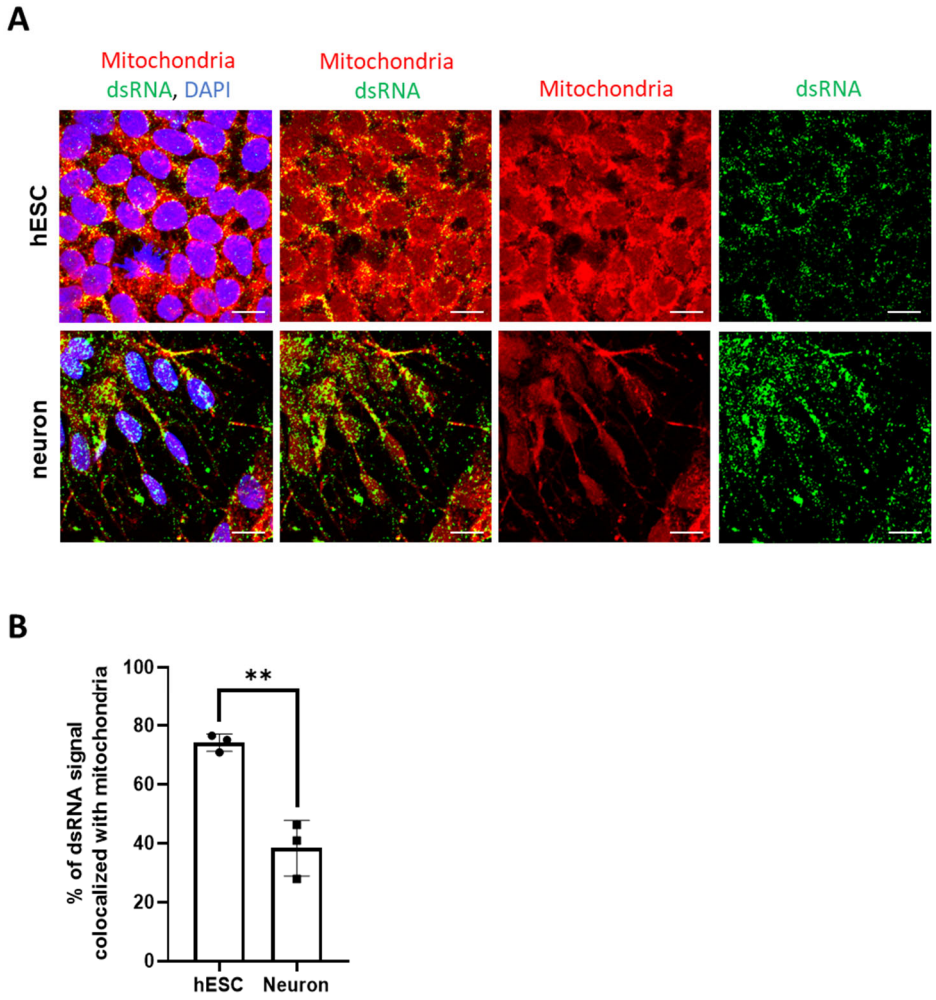

Fig. S7. Examining co-localization of dsRNA with mitochondria in hESCs and neurons. (**A**) Immunofluorescent imaging of hESCs and neurons stained with DAPI (blue), J2 (dsRNA, green), and MitoTracker (mitochondria, red). (**B**) Quantification of dsRNA signal that is colocalized with mitochondria from (A). Data are shown as mean (n=3). Student's T-test, *$p < 0.05$, **$p < 0.01$, ***$p < 0.001$, ****$p < 0.0001$. Scale bars represent 10μm.

A

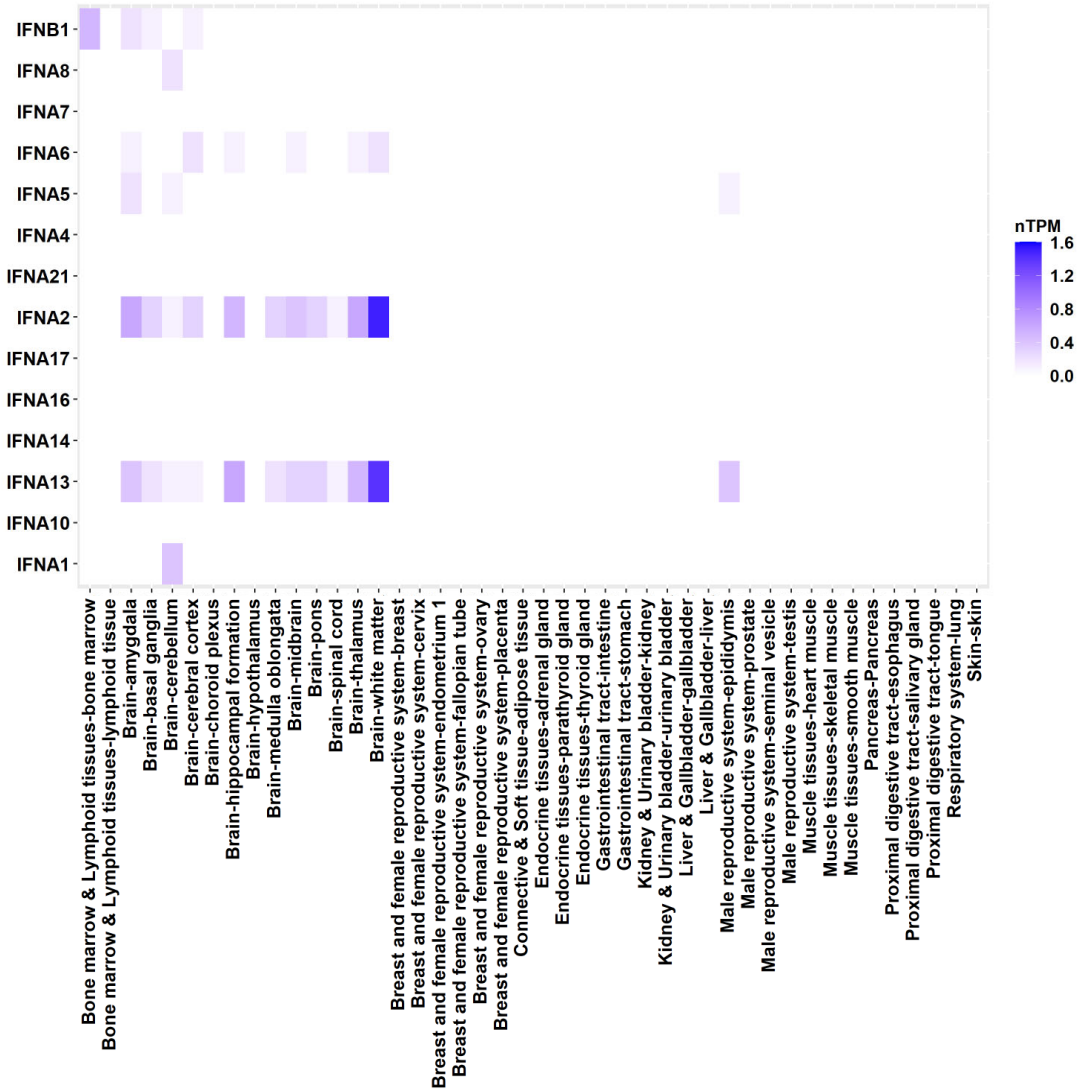

Fig. S8. RNA-Seq analysis of type I IFN in human tissues in the Human Protein Atlas (HPA) dataset. (**A**) Type I IFN (IFNβ and IFNα subtypes) expression in non-diseased tissue sites from 198 individuals analyzed by RNA-Seq. Data derived from the HPA database.

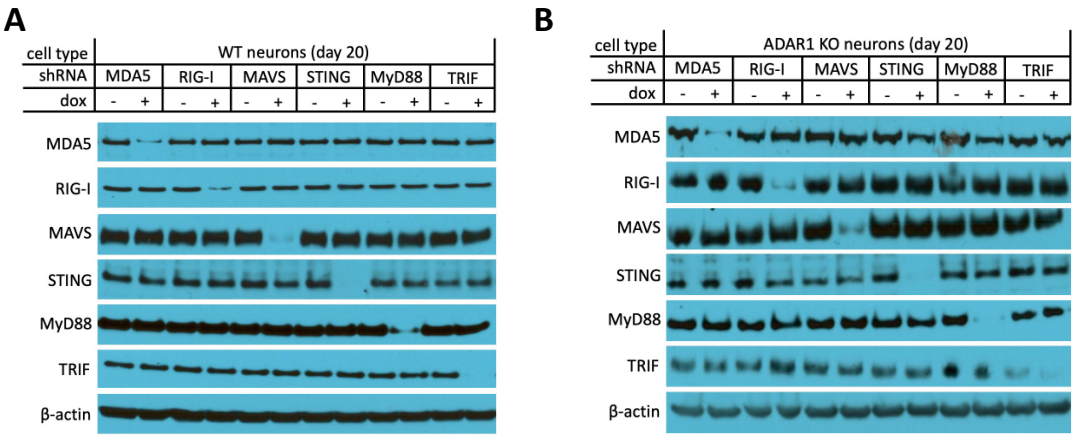

Fig. S9. shRNA mediated knockdown of protein expression in neurons. WT (**A**) and ADAR1 KO (**B**) neurons were transduced with lentiviruses containing doxycycline-inducible shRNAs targeting MDA5, RIG-I, MAVS, STING, MyD88, and TRIF. After mock or doxycycline (dox) treatment, neurons were harvested for western blot to confirm successful knockdown of each gene.

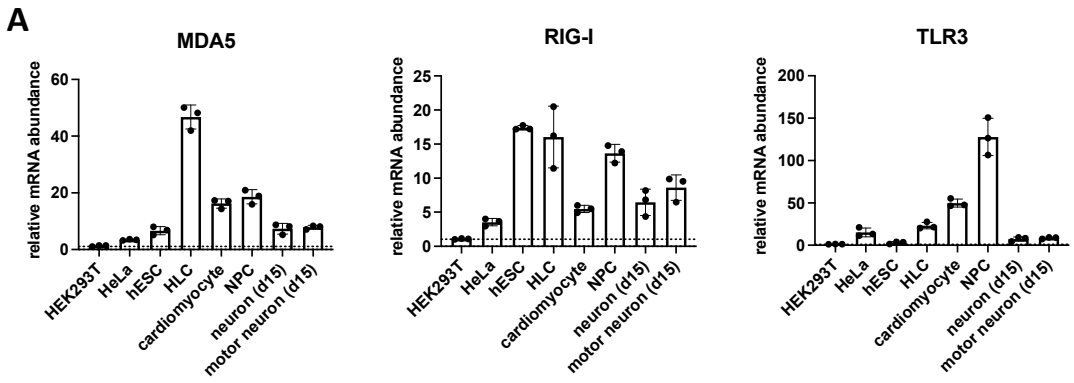

Fig. S10. Comparing PRR expression levels in diverse human cell types. (**A**) MDA5, RIG-I, and TLR3 mRNA levels measured in diverse human cell types via qPCR and normalized to levels in HEK-293T cells. *RPS11* used as a housekeeping gene for qPCR analysis. HLCs (hepatocyte-like cells), cardiomyocytes, NPCs (neural progenitor cells), neurons, and motor neurons were all derived from WT hESCs (HUES8). Neuron and motor neuron harvested at d15 (day 15 post-differentiation). All data presented as mean ± S.D (n=3).

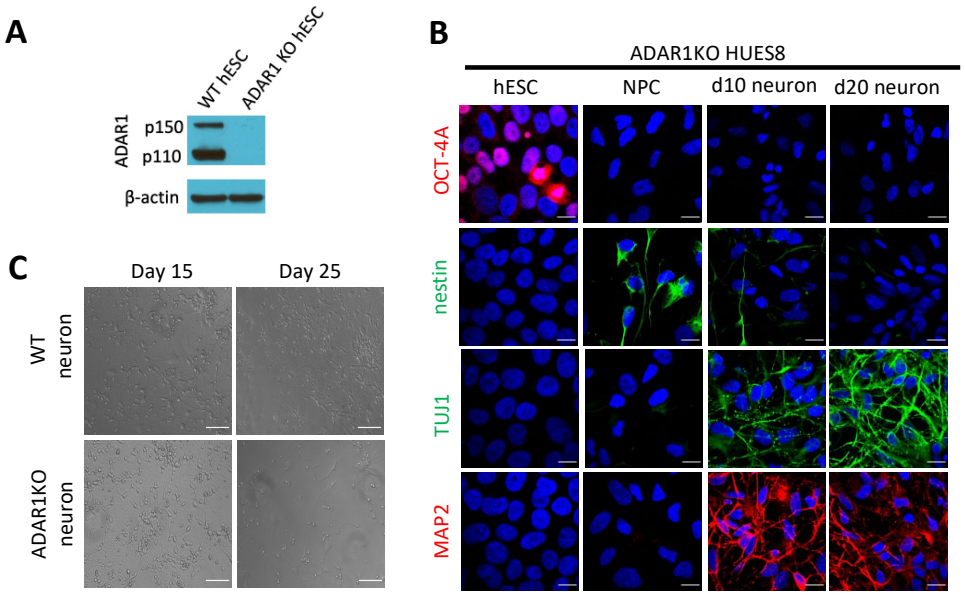

Fig. S11. Loss of ADAR1 in hESCs does not interfere with NPC and neuron differentiation but induces neuronal death by day 25 post-differentiation. (**A**) Western blot of wildtype (WT) and ADAR1 KO HUES8 hESCs showing effective knockout of both ADAR1 isoforms, p110 and p150. (**B**) WT and ADAR1 KO hESCs (HUES8) were differentiated to neurons in parallel and imaged side-by-side. Differentiation of WT hESC presented in Fig. S1A, and differentiation of ADAR1 KO hESC presented here in Fig. S11B. Cells stained for a hESC marker (OCT-4A), a neural progenitor cell (NPC) marker (nestin), and neuron markers (TUJ1 and MAP2). Comparing hESC to neuron differentiation between Fig. S1A (WT) and Fig. S11B (ADAR1 KO) demonstrates that there is no difference in neuronal differentiation between WT and ADAR1 KO hESCs. (**C**) Brightfield images of WT and ADAR1 KO neurons at day 15 and day 25 post-differentiation. Scale bars represent 10μm in (B) and 50μm in (C).

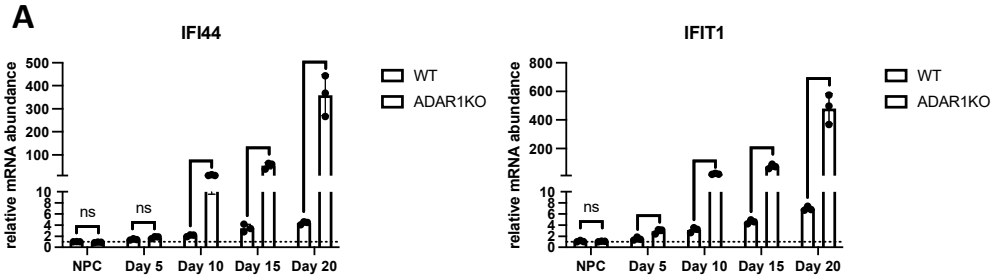

Fig. S12. ADAR1 KO neurons express higher levels of ISGs than WT neurons. (**A**) *IFI44* and *IFIT1* mRNA levels measured in WT and ADAR1 KO neurons over the course of differentiation. *RPS11* used as a housekeeping gene for qPCR analysis. All data presented as mean ± S.D (n=3). Two-way ANOVA with Tukey corrected multiple comparisons, *p < 0.05, **p < 0.01, ***p < 0.001, ****p < 0.0001.

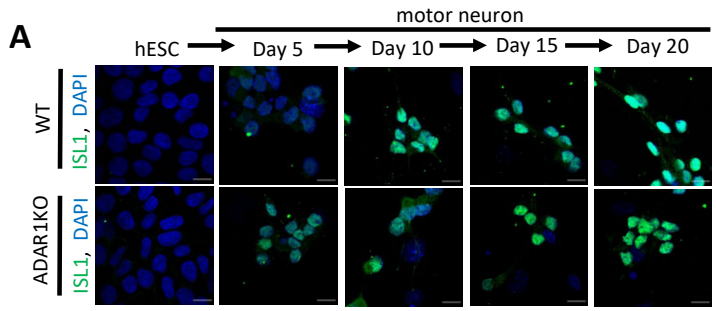

Fig. S13. Loss of ADAR1 does not disrupt expression of the motor neuron marker ISL1. (**A**) WT and ADAR1 KO hESCs were differentiated to motor neurons via embryoid bodies in cell suspension. Neurons were stained with the motor neuron specific marker ISL1 (green) or DAPI (blue) at different stages of differentiation (A). Scale bars represent 10μm.

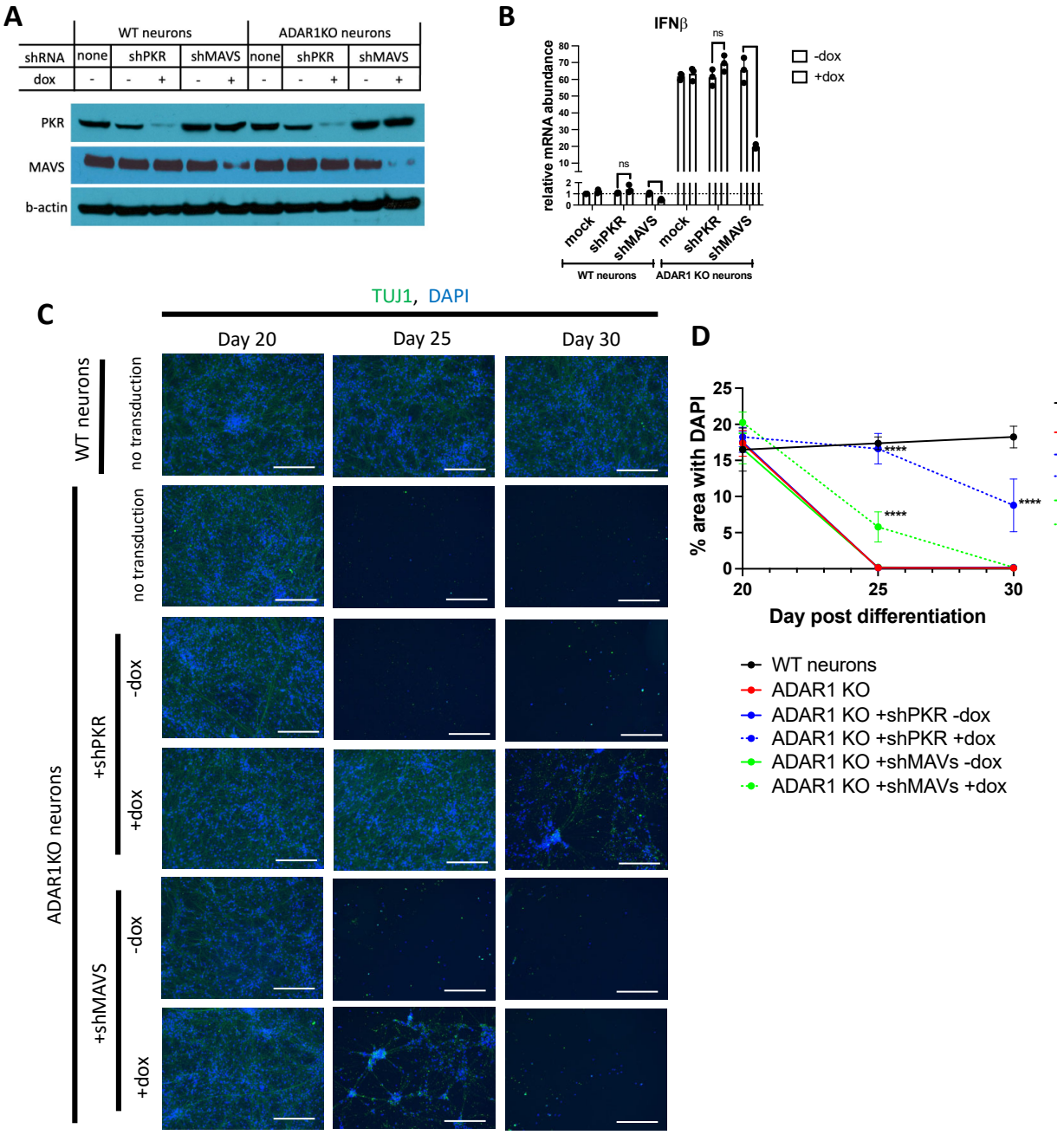

Fig. S14. PKR activation and IFN production play a major and minor role in ADAR1 KO neuron death, respectively. (**A-D**) WT and ADAR1 KO neurons were transduced with lentivirus carrying a doxycycline (dox)-inducible shRNA for either PKR or MAVS. (A) Western blot confirming knockdown of PKR and MAVS. (B) qPCR of IFNβ transcript levels following doxycycline-induced knockdown of the indicated genes. *RPS11* used as housekeeping gene. (C) Immunofluorescent images of WT and ADAR1 KO neurons with knockdown of the indicated genes at 20, 25, and 30 days post differentiation stained for TUJ1 (green) and DAPI (blue). (D) Cell survival measured by percent area covered by DAPI in images from (C). All quantified data shown are mean ± S.D (n=3 in B, n=6 in D). Two-way ANOVA with Tukey corrected multiple comparisons, *p < 0.05, **p < 0.01, ***p < 0.001, ****p < 0.0001. Scale bars represent 10μm.

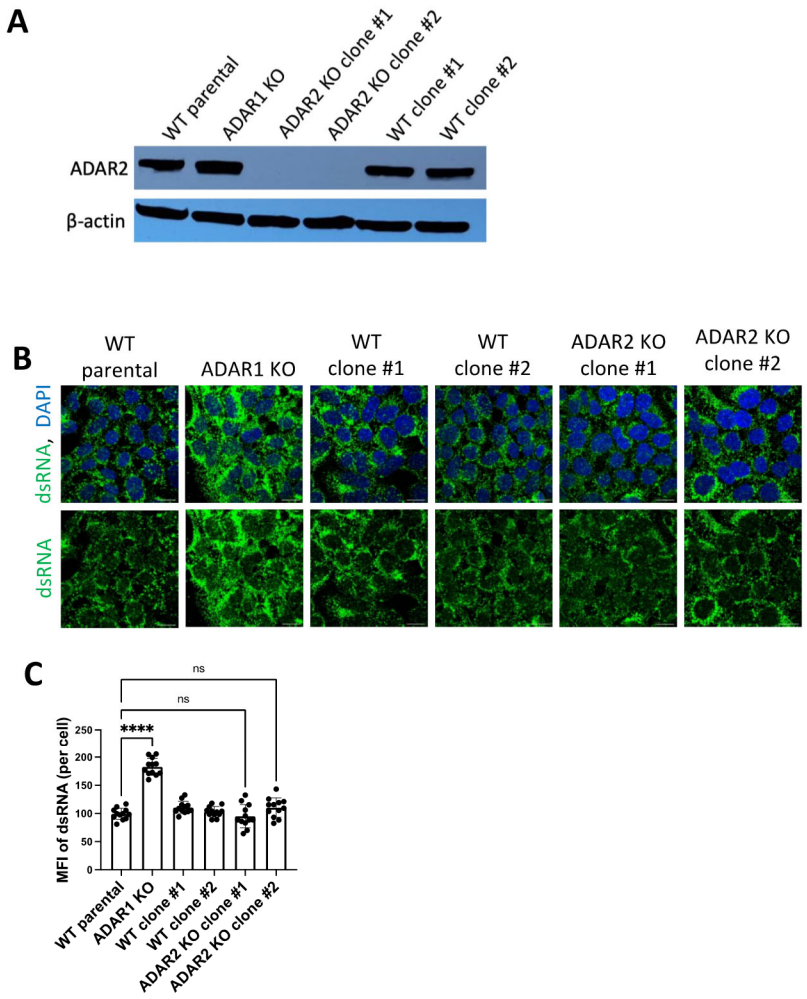

Fig. S15. Loss of ADAR2 does not increase dsRNA burden in HEK-293T cells. (**A**) Western blot of WT, ADAR1 KO, and ADAR2 KO HEK-293T cells confirming knockout of ADAR2. (**B**) Immunofluorescent imaging of WT, ADAR1 KO, and ADAR2 KO HEK-293T cells stained with DAPI (blue) and J2 (dsRNA, green). (**C**) Quantification of dsRNA signal from (B). All quantified data shown are mean ± S.D (n=12). One-way ANOVA with Tukey corrected multiple comparisons. *$p < 0.05$, **$p < 0.01$, ***$p < 0.001$, ****$p < 0.0001$. All scale bars represent 10μm.

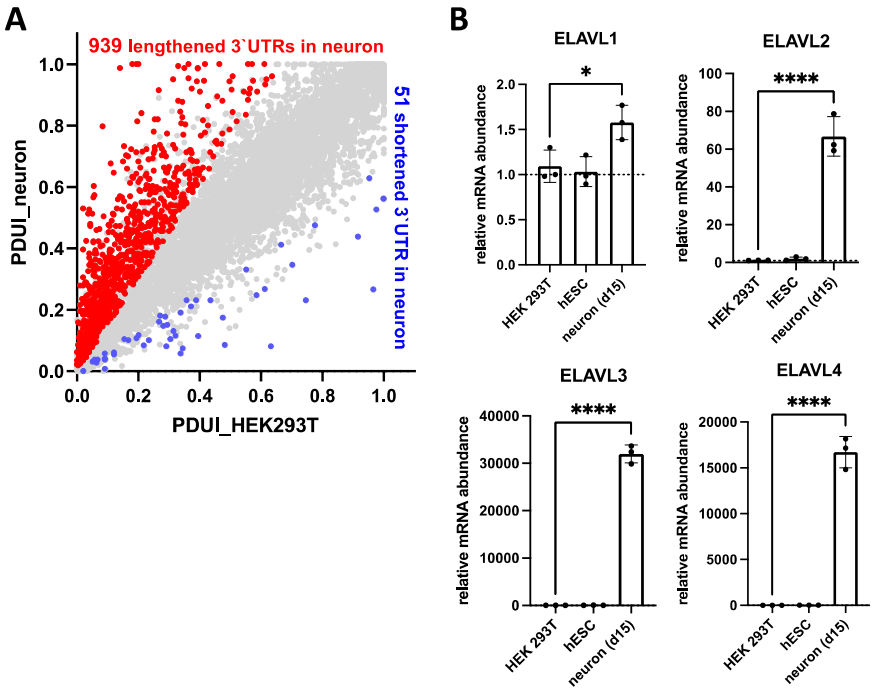
A
939 lengthened 3`UTRs in neuron
51 shortened 3`UTR in neuron
PDUI_neuron
PDUI_HEK293T
0.0
0.2
0.4
0.6
0.8
1.0
B
ELAVL1
ELAVL2
ELAVL3
ELAVL4
relative mRNA abundance
*
****
HEK 293T
hESC
neuron (d15)

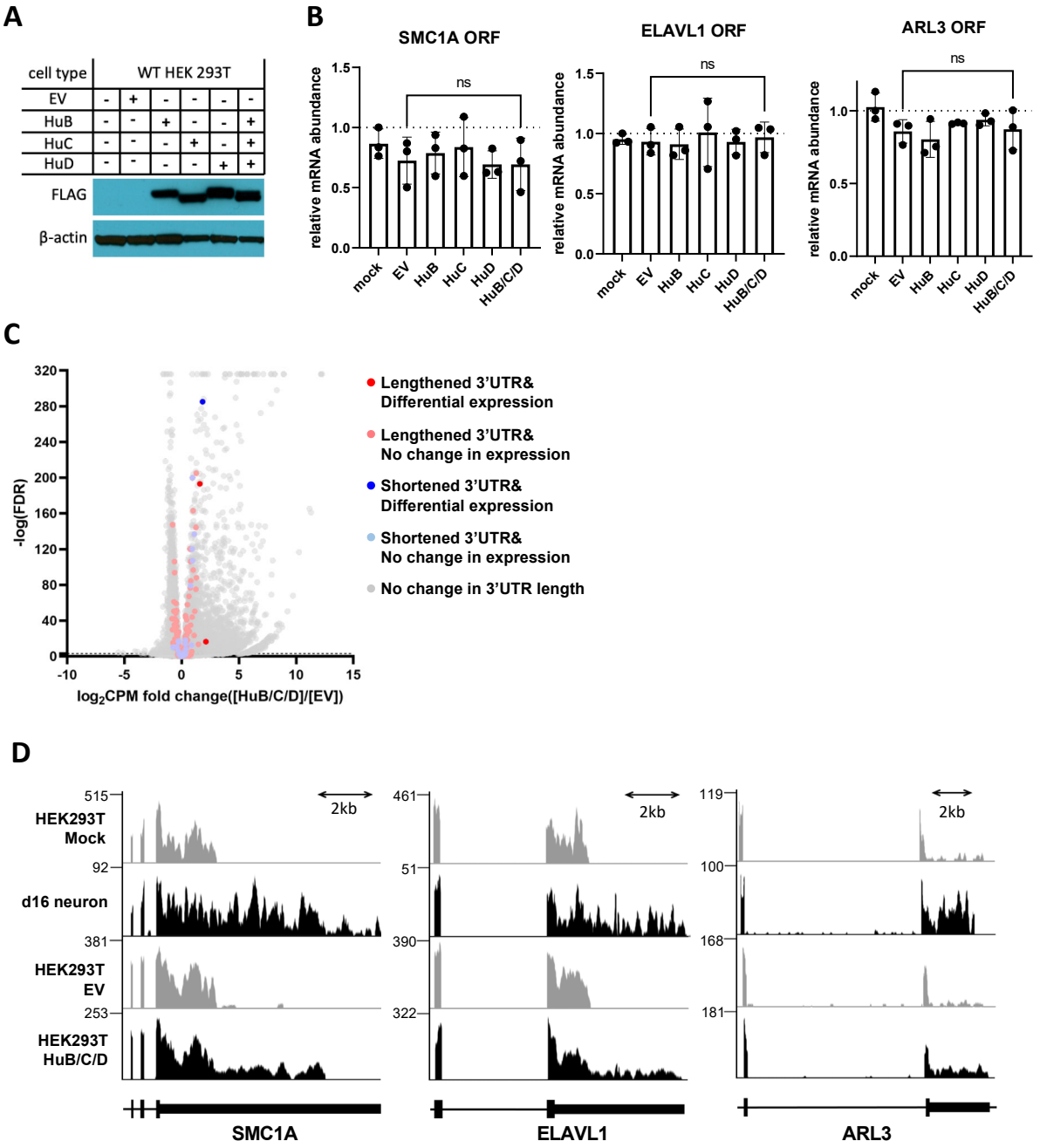

Fig. S17. Ectopic expression of HuB, HuC, and HuD in HEK-293T: Total transcript levels of the 3'UTR lengthened genes remain predominantly constant. (**A**) Western blot demonstrating expression of FLAG tagged HuB, -C, -D in HEK-293T cells. EV, empty vector. (**B**) qPCR data showing total transcript expression of genes in Fig. 4A. Primers detect a region in the open reading frame (ORF). *RPS11* used as a housekeeping gene for qPCR analysis. (**C**) Volcano plot showing

differential expression of genes between HEK-293T_EV (n=3) vs. HEK-293T_HuB/C/D cells (n=3). Genes whose 3'UTR is lengthened (dark red, light red) or shortened (dark blue, light blue) in HEK-293T_HuB/C/D cells are colored, which was determined by DaPars analysis in Fig. 4B; dark color dots indicate genes that are also significantly differentially expressed (CPM [counts per million] fold change ≥ 3, FDR ≤ 0.001). Note that most genes with altered 3'UTR length do not exhibit significant differences in transcript expression levels. Genes with no significant change in 3'UTR length and expression levels are in gray. (**D**) Distribution of sequencing reads for select genes whose 3'UTR is lengthened in day 16 (d16) post-differentiation neuron and HEK-293T_HuB/C/D cells. Numbers on y-axis indicate RNA seq read coverage. All quantified data shown are mean ± S.D (n=3). One-way ANOVA with Tukey corrected multiple comparisons, *p < 0.05, **p < 0.01, ***p < 0.001, ****p < 0.0001.

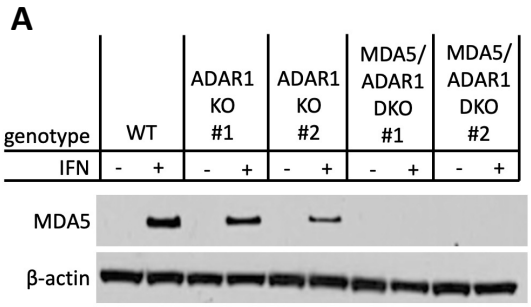

Fig. S18. Generation of ADAR1/MDA5 double-knockout (DKO) cells. (**A**) Western blot demonstrating effective knockout of MDA5 in ADAR1 KO HEK-293T cells. Clone #1 was used in experiments for Fig. 4.

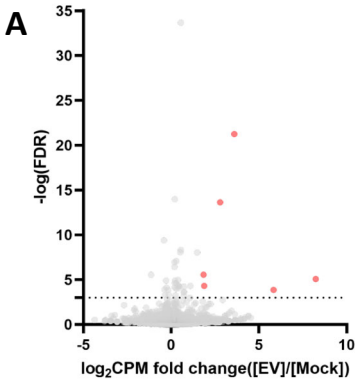

Fig. S19. Transcriptomic changes between mock and empty vector (EV) transfected HEK-293T cells. (**A**) Volcano plot showing differential expression of genes between WT HEK-293T_Mock (n=3) vs. WT HEK-293T_EV cells (n=3). Upregulated genes (red; FDR ≤ 0.001, CPM [counts per million] fold change ≥ 3) and downregulated genes (blue; FDR ≤ 0.001, CPM fold change ≤ 0.333) are colored. In contrast to Fig. 5A, most genes are not differentially expressed.

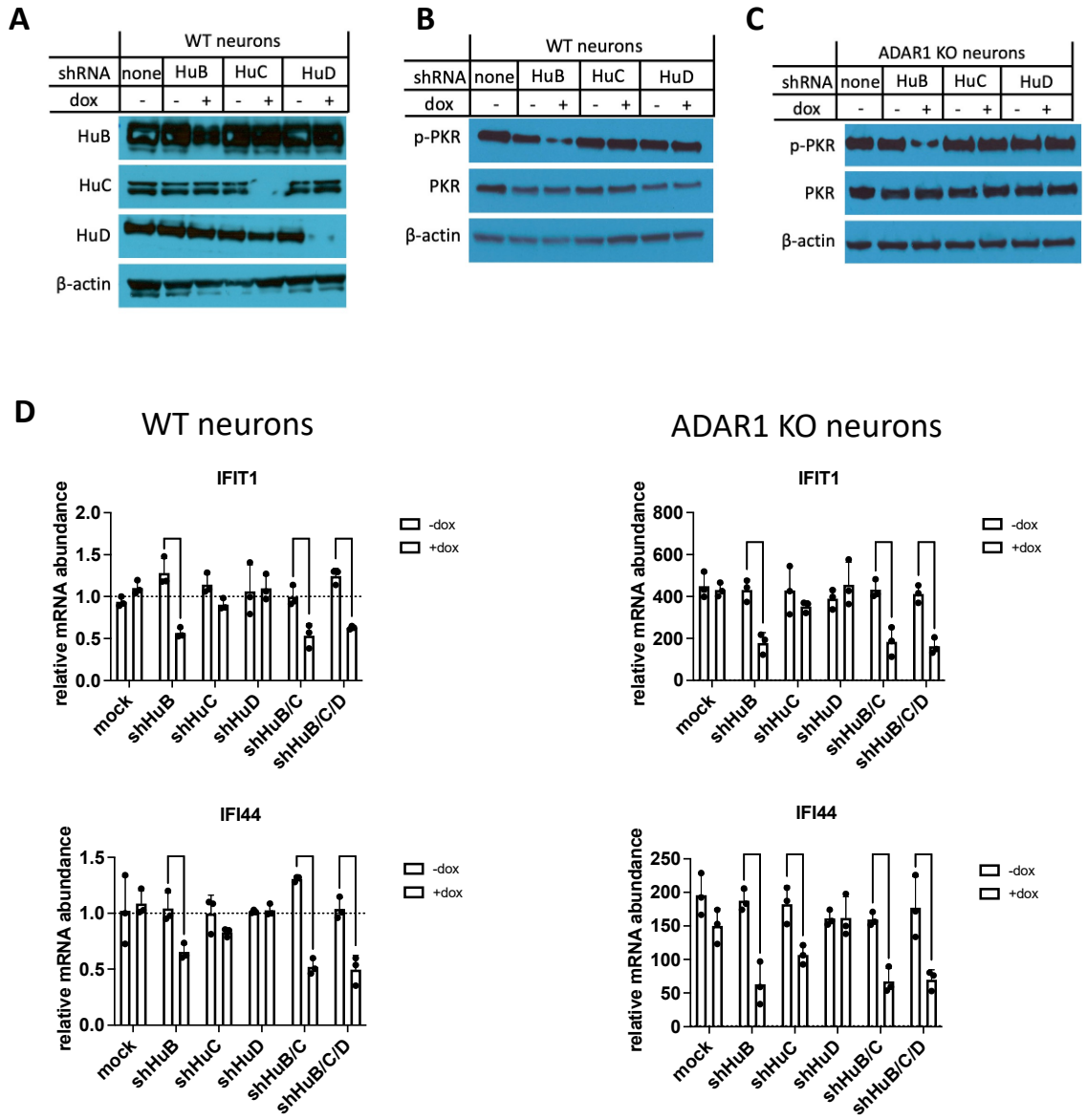

Fig. S20. Knockdown of ELAVL proteins in neurons reduces PKR activation and ISG expression (**A**) Western blot demonstrating effective knockdown of HuB, HuC, and HuD in neurons using doxycycline (dox) inducible shRNAs. (**B-C**) Western blot measuring PKR activation in WT (B) and ADAR1 KO (C) neurons with indicated ELAVL protein depleted. p-PKR, phosphorylated PKR. (**D**) qPCR of ISGs (*IFIT1* and *IFI44*) in WT and ADAR1 KO neurons following depletion of the indicated ELAVL proteins. All quantified data shown are mean ± S.D (n=3). Two-way ANOVA with Tukey corrected multiple comparisons, *p < 0.05, **p < 0.01, ***p < 0.001, ****p < 0.0001.

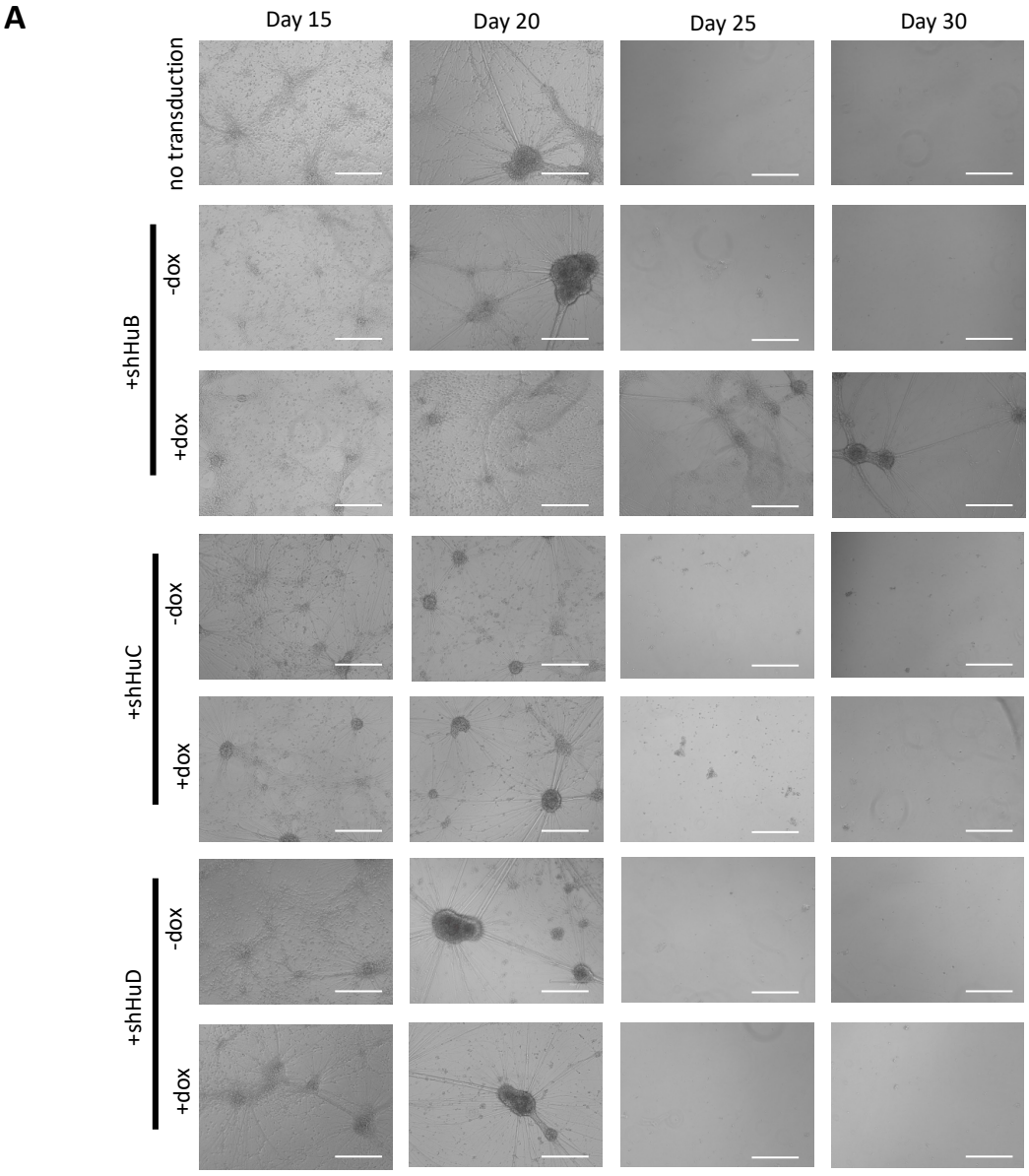

Fig. S21. Depletion of HuB can prolong the survival of ADAR1 KO neurons (**A**) Brightfield images of ADAR1 KO neurons with doxycycline-inducible knockdown of HuB, -C, or -D at 15, 20, 25, and 30 days post differentiation. Images are representative of three biological triplicates. Scale bars represent 400µm.

Table S1: Primers used for qRT-PCR (qPCR).

Gene Name	Forward	Reverse
ND1	CCACCTCTAGCCTAGCCGTTTA	GGGTCATGATGGCAGGAGTAAT
CYTB	ATCACTCGAGACGTAAATTATGGCT	TGAACTAGGTCTGTCCCAATGTATG
IFIT1	ACACCTGAAAGGCCAGAATG	GGTTTTCAGGGTCCACTTCA
PKR	TGGAAAGCGAACAAGGAGTAAG	CCATCCCGTAGGTCTGTGAA
β-actin	CACCATTGGCAATGAGCGGTTC	AGGTCTTTGCGGATGTCCACGT
HSPA4	TGTACCCCGGCCTGTATATCA	ACGTTCGTGACTATCTGGCTC
IFNβ	GTCAGAGTGGAAATCCTAAG	ACAGCATCTGCTGGTTGAAG
Pan-IFNα	GTGAGGAAATACTTCCAAAGAATCAC	TCTCATGATTTCTGCTCTGACAA
IFNα21	TGGTGCTCAGCTACAAATCC	CCCATTTGTGCCAGGAGTAT
IFNλ1	CACATTGGCAGGTTCAAATCTCT	CCAGCGGACTCCTTTTTGG
MDA5	AGCTGACACTTCCTTCTGCC	GGGGCATGGAGAATAACTCA
RIG-I	CCTACCTACATCCTGAGCTACAT	TCTAGGGCATCCAAAAAGCCA
TLR3	TTGCCTTGTATCTACTTTTGGGG	TCAACACTGTTATGTTTGTGGGT
SMC1A ORF	CATCAAAGCTCGTAACTTCCTCG	CCCCAGAACGACTAATCTCTTCA
SMC1A Long	TGTTAGCTGGACTGGCATAAG	ACATTCTGCCTCCCTGAAAG
ELAVL1 ORF	AACTACGTGACCGCGAAGG	CGCCCAAACCGAGAGAACA
ELAVL1 Long	CTGGGACAGGTGAGAAGAAAC	AAACAGCGGAGACCACATAC
ARL3 ORF	CCTGGGCTTGGATAATGCTGG	AACCCTGTGTAGGTGTGATGT
ARL3 Long	CAGAAGCCACTCCTCTGATAAC	GGGCTCAAAGGGAAGATGAA
BCDIN3D ORF	CTCGACGTGGGGTGTAACTC	GTTTCCCCGTCAGGTAGGG
BCDIN3D Long	ACTTGTTAGACTGGAGGCTTATG	CACTGAAGCTGGACTCCTTATT
ELAVL2	CAACACCCTGAATGGATTGAGA	TTTTTGGAAGTCCGCTGACAT
ELAVL3	TCGAGTCCTGCAAGTTGGTTC	TGCATCATTGGGGTCAGAATAGT
ELAVL4	AACCTCTATGTTAGCGGCCTT	TGGACACTCCTGTGACTTGAT
RPS11	GCCGAGACTATCTGCACTAC	ATGTCCAGCCTCAGAACTTC
ZIKV	TTGGTCATGATACTGCTGATTGC	CTTGTGTTGGGCAACGACTG
18S	AACCCGTTGAACCCCATT	CCATCCAATCGGTAGTAGCG
IFIT1	ACACCTGAAAGGCCAGAATG	GGTTTTCAGGGTCCACTTCA
IFI44	GGTGGGCACTAATACAACTGG	CACACAGAATAAACGGCAGGTA
ANGPTL1	AGTGGACACTGGACATTGCAG	GCTTCCTCTTTACCATCTGTGG
STAT1	AGGAAAAGCAAGCGTAATCTTCA	TATTCCCCGACTGAGCCTGAT

Data file S1. (separate file) Alternative polyadenylation site analysis using DaPars2. DaPars2 uses RNA sequencing data to detect 3'UTR alternative polyadenylation sites and produce a PDUI (Percentage of Distal poly-A sites Usage Index) value for each gene. PDUI values derived from HEK-293T_Mock, HEK-293T_EV, HEK-293T_HuB/C/D, and neurons are listed (n=3 for all groups). EV, empty vector.

Data file S2. (separate file) Gene expression data for HEK-293T_Mock, HEK-293T_EV, and HEK-293T_HuB/C/D. N=3 for all groups. Gene expression comparisons of HEK-293T_EV vs. HEK-293T_HuB/C/D and HEK-293T_Mock vs. HEK-293T_EV. CPM (counts per million) values listed. Differential gene expression analysis conducted using edgeR. EV, empty vector

Data file S3. (separate file) Raw data file.